

PROCEEDINGS OF SPIE

[SPIDigitalLibrary.org/conference-proceedings-of-spie](https://spiedigitallibrary.org/conference-proceedings-of-spie)

Comparison of Sentinel-2 and Landsat-8 OLI satellite images vs. high spatial resolution images (MIVIS and WorldView-2) for mapping *Posidonia oceanica* meadows

Luigi Dattola, Sante Francesco Rende, Rocco Dominici, Pasquale Lanera, Rossella Di Mento, et al.

Luigi Dattola, Sante Francesco Rende, Rocco Dominici, Pasquale Lanera, Rossella Di Mento, Simone Scalise, Piero Cappa, Teresa Oranges, Giovanni Aramini, "Comparison of Sentinel-2 and Landsat-8 OLI satellite images vs. high spatial resolution images (MIVIS and WorldView-2) for mapping *Posidonia oceanica* meadows," Proc. SPIE 10784, Remote Sensing of the Ocean, Sea Ice, Coastal Waters, and Large Water Regions 2018, 1078419 (10 October 2018); doi: 10.1117/12.2326798

SPIE.

Event: SPIE Remote Sensing, 2018, Berlin, Germany

Comparison of Sentinel-2 and Landsat-8 OLI satellite images vs. high spatial resolution images (MIVIS and WorldView-2) for mapping *Posidonia oceanica* meadows

Luigi Dattola ^{*a}, Sante Francesco Rende^b, Rocco Dominici^c, Pasquale Lanera^b, Rossella Di Mento^b, Simone Scalise^d, Piero Cappa^d, Teresa Oranges^a and Giovanni Aramini^e

^aARPACAL - Regional Agency for the Environmental Protection (Calabria);^bISPRA - Italian National Institute for Environment, (Roma);^cDepartment of Biology, Ecology and Earth Sciences - University of Calabria; ^dMPA – Marine Protected Areas Capo Rizzuto (Crotone - Italy); ^eRegione Calabria - Department of Environment and Territory - Parks and Protected Natural Areas;

*l.dattola@arpacal.it

ABSTRACT

Mediterranean seagrasses are represented by five species, whose most representative are *Posidonia oceanica* (L.) Delile and *Cymodocea nodosa* (Ucria) Ascherson. Spatial data analysis through remote sensing techniques is certainly a useful tool in order to understand and quantify the extent or loss of seagrass areas. Seagrass mapping and monitoring by remote sensing have been established using various optical remote sensors and mapping methods¹. In most studies for habitat mapping, the most common satellite images used are Landsat, Ikonos, Quickbird, Pleiades, World View 2 and the recent Sentinel-2 etc. ¹⁻². The aim of this work is to compare the spatial accuracy of medium – resolution satellite images (Sentinel-2 and Landsat-8 OLI) vs. high-resolution images (MIVIS and WorldView-2) for mapping *P. oceanica* meadows and evaluating their conservation status. The present study was conducted in 2016 within the MPA “Capo Rizzuto” (Mediterranean Sea - Southern Ionian Sea). Remote sensing images were processed following several stages such as preprocessing phase, segmentation, supervised classification and accuracy classification assessment. Preliminary results highlighted differences in spatial and thematic accuracy between medium and very high spatial resolution images for seagrass habitat mapping.

Keywords: Mediterranean seagrasses, *Posidonia oceanica*, *Cymodocea nodosa*, Ionian Sea, remote sensing

1. INTRODUCTION

Coastal habitat mapping has a crucial importance for the implementation of EU policies, especially for important habitats such as seagrass meadows. Seagrasses beds are among the planet’s most effective natural ecosystems for capturing and storing carbon (C); however, if degraded, they could release stored C into the atmosphere and accelerate global warming. Consequently, the management of these important resources is a priority. Spatial data analysis through remote sensing techniques is certainly a useful tool in order to understand and quantify the extent or loss of seagrass areas¹. Compared with conventional techniques, remote sensing can provide synoptic coverage over a range of spatial resolutions (coarse to fine), at regular temporal frequencies, to facilitate monitoring of coastal environments². *P. oceanica* species is protected by legislation under the EU Habitat Directive (92/43/CEE), the Bern (Annex II, Strictly Protected Flora Species) and the Barcelona (dedicated Action Plan under the “Protocol concerning Specially Protected Areas and Biological Diversity in the Mediterranean”) Conventions as well as other legislations at a national level. Furthermore, according to the Marine Strategy Framework Directive (MSFD; 2008/56/EC), *P. oceanica* is selected as a representative species of the angiosperm quality elements for the Mediterranean marine environment and a ‘Good Environmental Status’ shall be achieved by all Member States regarding the angiosperm habitats. Currently, optical satellite remote sensing comprises one of the most important methods to detect, map and monitor seagrass ecosystems due to its time- and cost-effectiveness over large areas as well as remote locations ¹⁻³⁻⁴⁻⁵. Analysis of multivariate spaceborne remote sensing data allows retrospective quantitative assessment of seagrass meadows⁶⁻⁷. Focusing on the Mediterranean seagrass ecosystems, several studies have utilized satellite imagery to map the distribution of the dominant *P. oceanica* ⁸⁻⁹⁻¹⁰. Seagrass mapping and monitoring using remote sensing have been established using various optical remote sensors

(high-, moderate-, and low-spatial resolutions) and mapping methods¹. The aim of this work is to compare the spatial accuracy of medium – resolution satellite images (Sentinel-2 and Landsat-8 OLI) vs. high-resolution images (MIVIS and WorldView-2) for mapping *P. oceanica* meadows and evaluating their conservation status.

2. MATERIALS AND METHODS

2.1 Area of study

This research was conducted in the Marine Protected Area (MPA) of Capo Rizzuto, Southern Ionian Sea (Calabria) in 2016 (Figure 1). The MPA Capo Rizzuto encompasses roughly 13,500 hectares of open water, bordering 37 km of coastline. The field data were collected with a towing vehicle equipped with high-definition (HD) vertical camera¹¹.

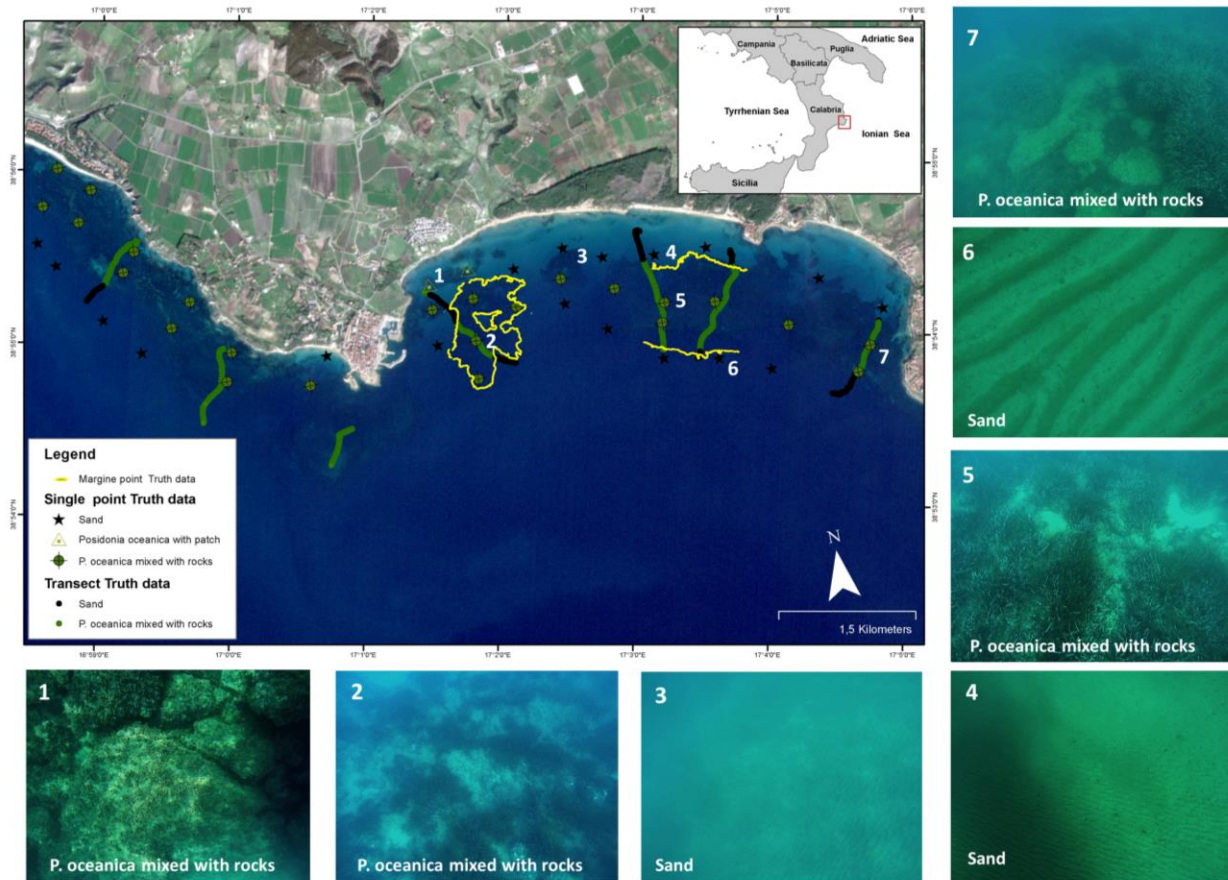


Figure 1. Study area located in the Marine Protected Area of Capo Rizzuto (KR, Italy) - located at 38°58'N / 17°13'E. Photographic representation of the truth data points.

2.2. Dataset

The high-resolution satellite imagery used in this study was acquired by World View 2 Multi Spectral (MS) image. The WorldView-2 satellite was launched on 8 October 2009 and is the first high-resolution satellite with 8 optical bands. WorldView-2 will simultaneously collect Panchromatic imagery at 0.46m and Multispectral imagery at 1.84m. The band 1 (Coastal Band) is useful for coastal studies (Figure 2A and 3A).

MIVIS images (Multispectral Infrared Visible Imaging Spectrometer) were acquired in August 2011 with an airborne Iperspectral (IS) platform. The MIVIS sensor, whiskbroom type, has a 2 mrad FOV, a high spectral resolution (0.02µm and 0.05 µm), a radiometric resolution of 12 bit and a spatial resolution of 3m. MIVIS acquires on 102 spectral bands in the regions of the electromagnetic spectrum of the visible, near infrared, middle and thermal infrared (Figure 2B and 3B).

The middle-resolution satellite imagery was acquired by Sentinel-2A, the first satellite of the twin polar-orbiting Sentinel-2 satellites. Sentinel-2A was launched on 23 June 2015 and have a Multi-Spectral Instrument (MSI) with 13 spectral bands that range from the visible range to the shortwave infrared (SWIR). Bands come in variable resolutions from 10 to 60 meter and their wavelength is determined based on specific purposes (Figure 2C and 3C). The other medium resolution satellite imagery was acquired by Landsat 8 OLI. The Landsat 8 OLI is an American Earth observation satellite launched on February 11, 2013 Landsat 8 Operational Land Imager (OLI) and Thermal Infrared Sensor (TIRS) images consist of nine Multispectral bands with a spatial resolution of 30 meters for Bands 1 to 7 and 9. The ultra blue Band 1 is useful for coastal studies (Figure 2D and 3D).

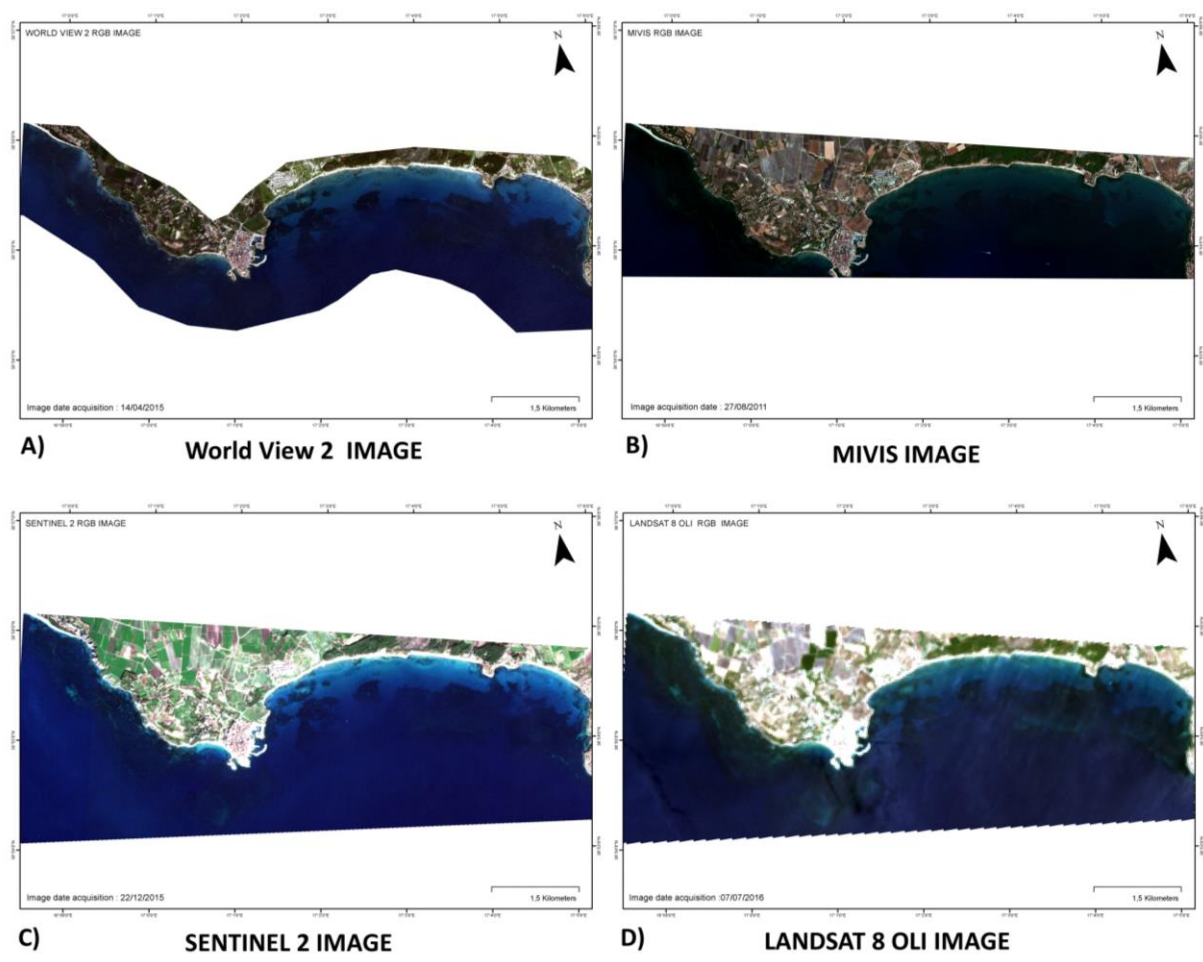


Figure 2. Multispectral and Iperspectral RGB images.

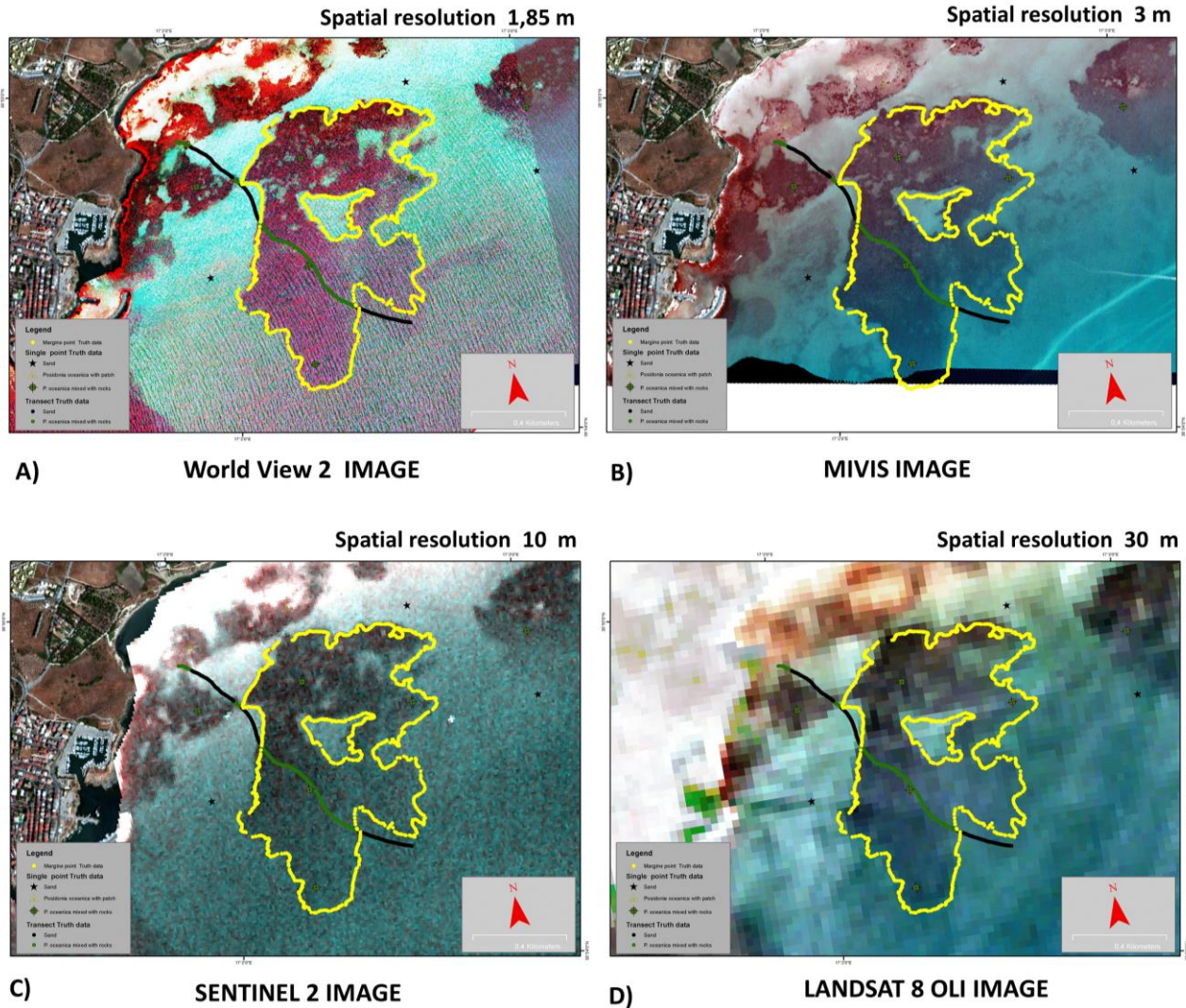


Figure 3. Comparison between spatial resolutions Multispectral and Iperspectral images.

2.3. Methodology

The Multispectral (MS) satellite images and Iperspectral (IS) airborne data has been processed following several stages such as: geometric correction, radiometric conversion, image segmentation and image enhancement. The radiometric conversion has consisted in the conversion of radiance to reflectance and the water column correction. In particular, the Water Column Correction (WCC), which was masked for land pixels, was developed by Lyzenga¹³ and applied on the radiometric corrected MIVIS, Worldview-2, SENTINEL II and LANDSAT 8 OLI images. (Figure 3 and 4). This method produces a depth invariant index from each pair of spectral bands of a multispectral dataset. The assumption is that the radiance ratios of two distinct benthic cover are independent for water depth as long as attenuation coefficients are the same in each couple bands. As a result, depth invariant index (DII) was generated for each couple bands following formula (1):

$$(1) \text{DII} = \text{Ln}[\text{Ri}] - [\text{ki/kj}] * \text{Ln}(\text{Rj})$$

Processing and image analysis has been performed through pixel-based supervised classification algorithms, using the Erdas and ArcGIS 10.3 software, Figure 4. The classification was performed using the following ecotipologies: i) Sand, ii) *P. oceanica* with patch, iii) *P. oceanica* mixed with rocks (Figure 5 and 6).

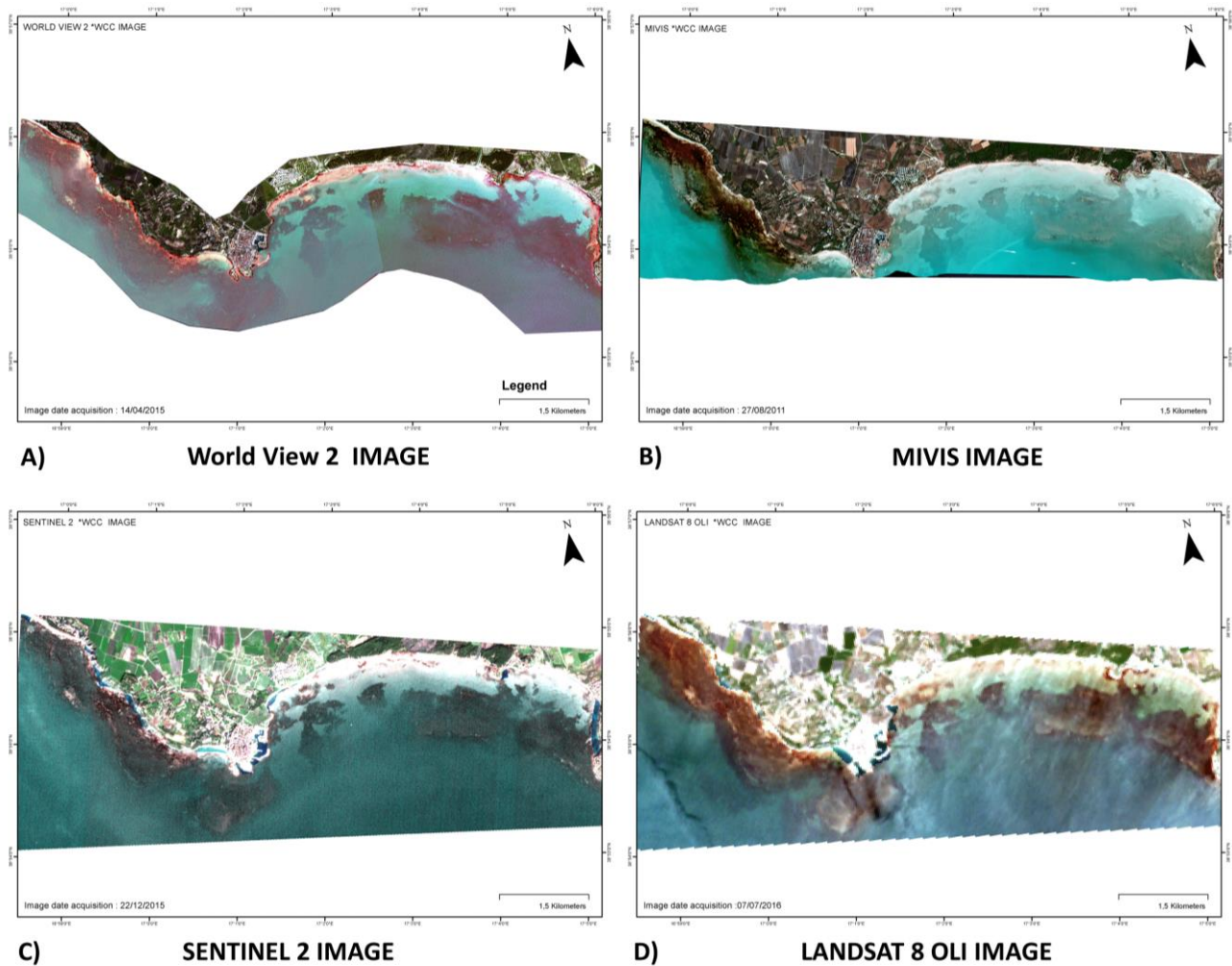


Figure 4. Multispectral and Iperspectral images after the water column correction.

2.4. Field data collection

Field data collection was carried with a towing vehicle equipped with high definition (HD) vertical camera¹¹. Images were processed by Structure From Motion (SfM) algorithms that allowed us to generate 2D and 3D models for identifying and classifying meadow physiographic and structural features¹². Images were used to instruct the classifier algorithm for ground - truth validation¹⁴⁻¹⁵. The spatial accuracy estimation was also performed using 1588 truth data points that were extracted from the margin of an area of interest covered by *P. oceanica* using as a basemap the multibeam grid executed in the study area in 2012 (Figure 5). The thematic accuracy estimation was also performed using 50 truth points arranged randomly (Figure 6), finally, an additional accuracy thematic estimation was performed using 13808 obtained from the orthogonal video transects (Figure 6).

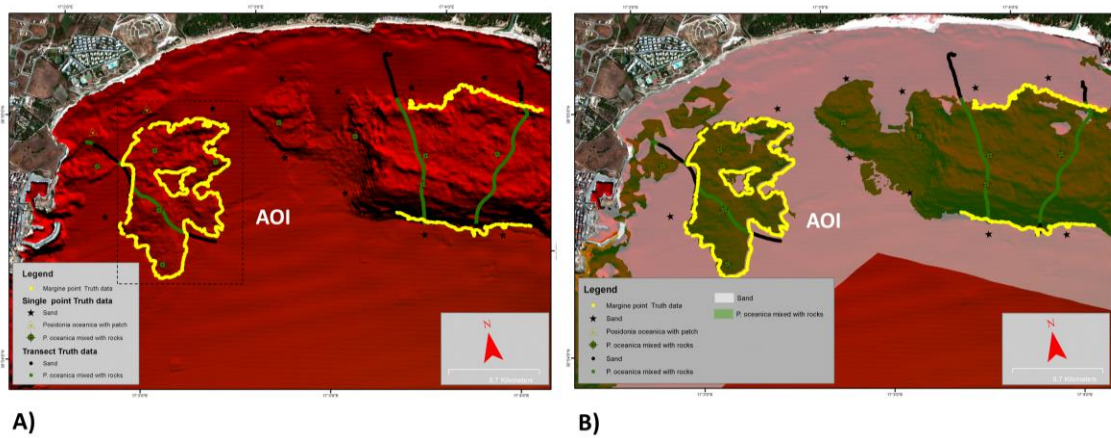


Figure 5. Truth data points at the edge of the area covered by *P. oceanica* with basemap the multibeam grid.

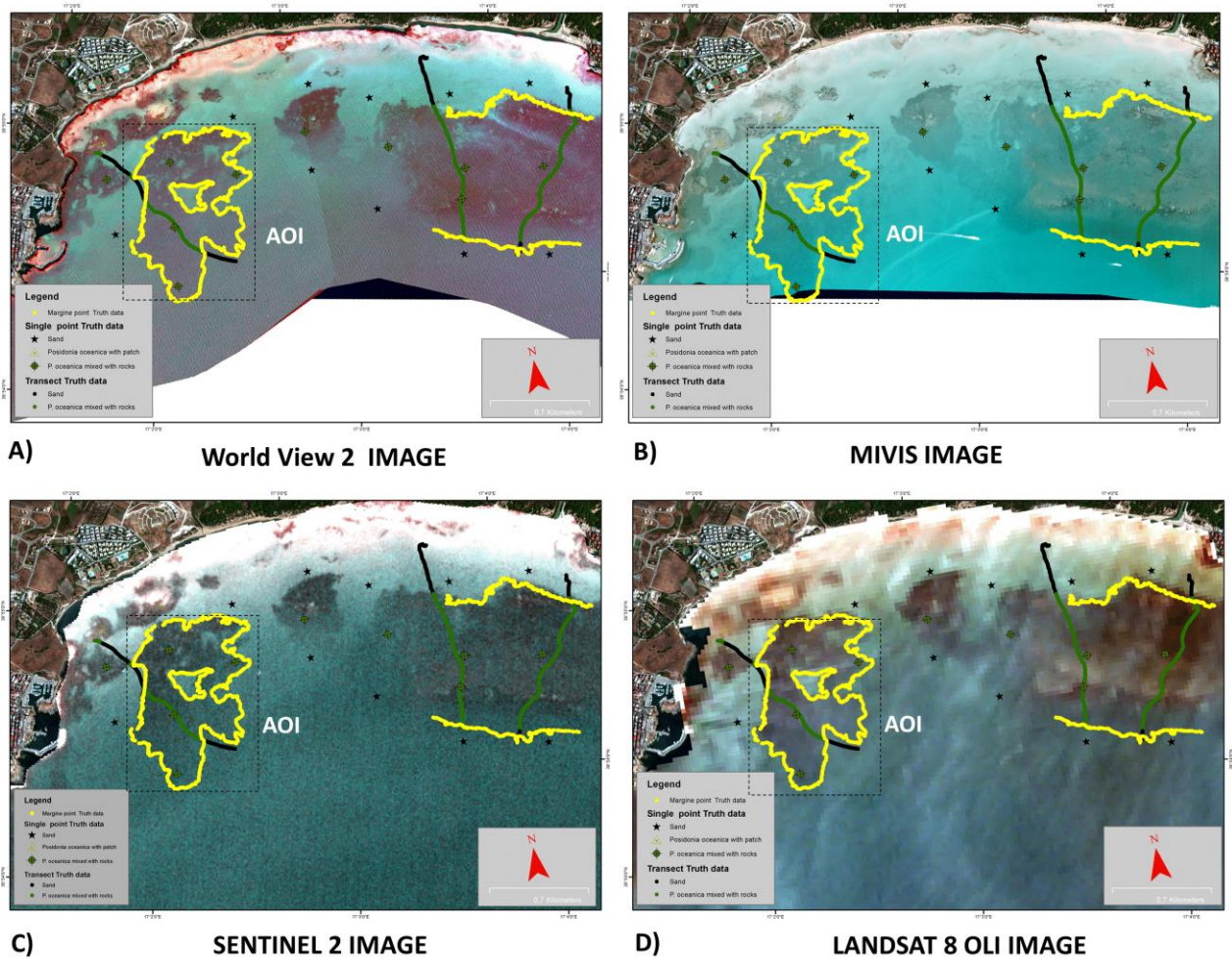


Figure 6. Correct images with the water column showing all truth data points for spatial and thematic accuracy estimation.

3. RESULTS

After pre-processing steps, we have obtained a series of correct images (MIVIS, World View 2, Sentinel 2 and Landsat 8 OLI) with the removing of the water column noise that enhances bottom features following the increase of the seabed spectral variability. Information for setting up the classifier training activity have been obtained from video - photographic inspections (Figure 6). The classification tool allowed us to obtain raster images of the bottom cover (Figure 6 and 7).

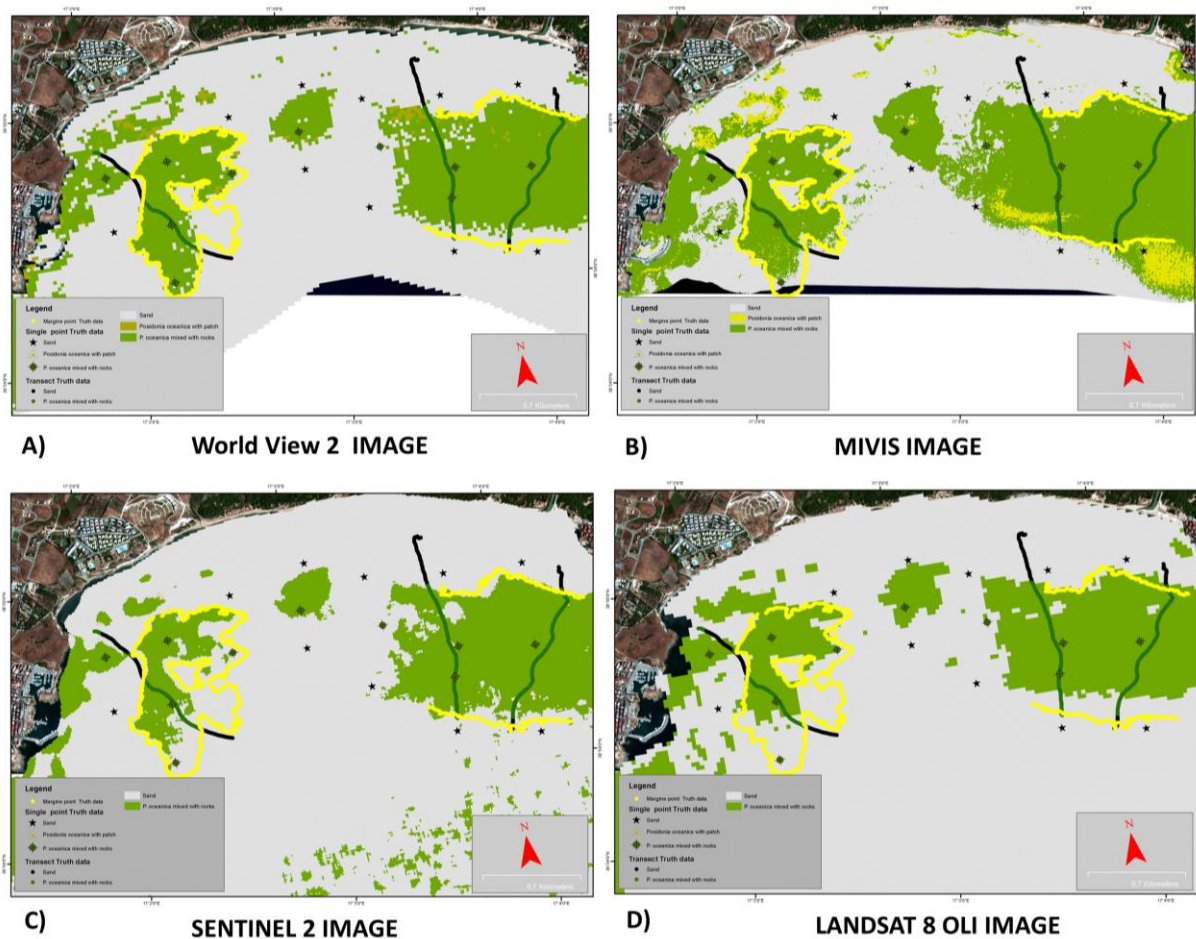


Figure 7. Comparison of classified raster images.

A preliminary comparison of the different processing activities (Figure 7 and 8) highlighted greater spatial accuracy of classification in MIVIS and World View 2 images than in Sentinel 2 and LANDSAT 8 OLI images (Figure 7 and Figure 8). Classifications obtained by MIVIS and World View 2 images are quite comparable, although sensors differ in terms of band number. Sentinel 2 images, despite having a spatial resolution of 10 m pixels, showed good quality and suitability for sea bottom reconstruction. Regarding the LANDSAT 8 OLI images, it is noteworthy that, compared to the satellite images of the World View 2 and the MIVIS IS Airborne Sensor, there is a significant loss of spatial and themed resolution, in relation to the low resolution of the pixel of 30m x 30m (Figure 7 and Figure 8).

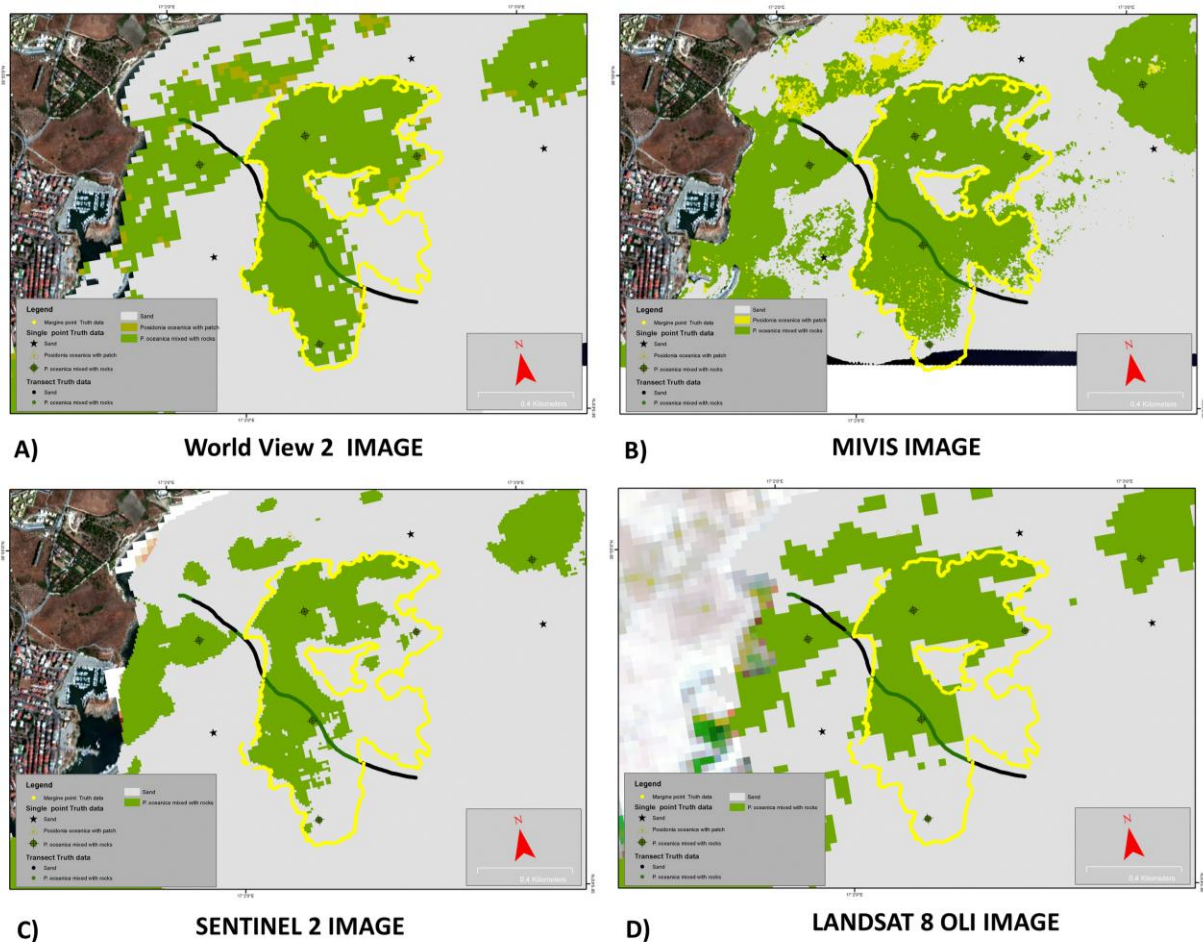


Figure 8. Comparison in an area of interest (AOI) between raster images classified.

The verification of the spatial and thematic accuracy of image classification was obtained by calculating the confusion matrices that summarize the correspondence between the truth data of the open field and the classified data 14 (Table 1, 2 and 3).

Table 1. Comparison of spatial accuracy (%) of bottom-type identification (1588 truth margin data point).

Thematic Class	World View 2	MIVIS	Sentinel 2	Landsat 8
Sand	95.45	73.68	90.91	100.00
P. oceanica with patch	0.00	50.00	0.00	0.00
P. oceanica mixed with rocks	92.00	100.00	84.00	88.00
Total Accuracy	88.00	86.05	82.00	87.76
Kappa	77.26	74.33	66.04	76.96

The confusion matrices were generated on the basis of the three types of truth data (margin points, random points, and transect points). The evaluation of the total spatial accuracy performed with the margin point area, assessed with the 1588 margin truth points, is greater for the MIVIS IS image (Table 1). The total thematic accuracy, assessed with the 50

random truth points and with the 13808 truth transect data point, shows higher values for the World View 2 and for the Landsat 8 images (Table 2 and Table 3).

Table 2. Comparison of thematic accuracy (%) of bottom-type identification (50 truth random data point).

Thematic Class	World View 2	MIVIS	Sentinel 2	Landsat 8
Sand	84.95	48.03	77.11	90.21
P. oceanica mixed with rocks	90.91	98.37	93.47	91.37
Total Accuracy	88.80	77.67	87.68	90.96
Kappa	75.77	50.88	72.37	80.50

Table 3. Comparison of thematic accuracy (%) of bottom-type identification (13808 truth transect data point).

Thematic Class	World View 2	MIVIS	Sentinel 2	Landsat 8
Sand	98.32	82.35	100.00	92.44
P. oceanica mixed with rocks	36.76	58.86	23.76	39.48
Total Accuracy	41.37	60.67	29.47	43.45
Kappa	7.91	13.29	4.46	7.26

4. DISCUSSION AND CONCLUSIONS

The results of the preliminary study allowed us to examine the differences in quality and spatial and thematic resolution obtained from medium resolution images to very high spatial resolution (Figure 7 and Figure 8). High-resolution MS satellite and airborne IS images, such as World View 2 or MIVIS images, are more accurate and thus more effective than medium resolution images in obtaining mapping products, mapping elements at local spatial scale, and estimating parameters such as habitat coverage, extension, produced biomass (Figure 9 and Table 1,2,3). Medium resolution MS satellite imagery, such as Sentinel 2 and LANDSAT 8 OLI images, may have application limits when accurate cartographic detail standards are required. However, for local-level mappings, the Sentinel 2 and Landsat 8 image they are still valid (Figure 7, Figure 8 and 9) ¹⁻¹⁶⁻¹⁷. Regarding LANDSAT 8 OLI satellite images, although they have 30m resolutions (Figure 7,8 and 9), they can still be used for mapping on a regional scale and to assess the presence/absence of submerged marine vegetation ¹. The resulted maps demonstrated the ability of Remote Sensing for producing spatially extensive maps and allowed quantitative estimation of seagrass coverage, accretion/erosion, and assessment of changes in MPA areas or Natura 2000 sites ¹⁸.

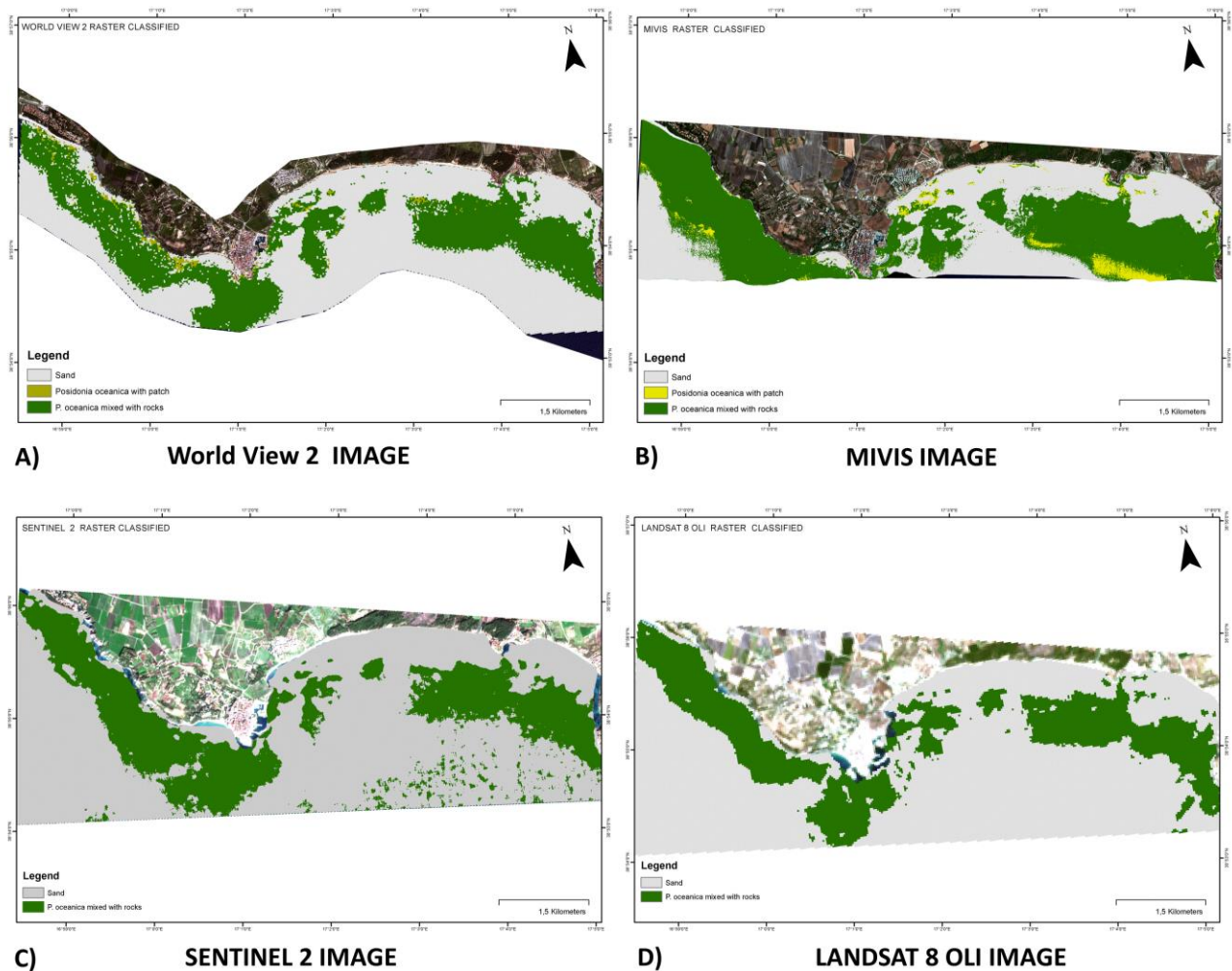


Figure 9. Classified Raster Images.

REFERENCES

- [1] Hossain, M. S., Bujang, J. S., Zakaria, M. H., and Hashim, M., "The application of remote sensing to seagrass ecosystems: an overview and future research prospects," *Int. J. Remote Sens.* **36**(1), 61-114 (2015).
- [2] Hossain, M. S., Bujang, J. S., Zakaria, M. H., and Hashim, M., "Application of Landsat images to seagrass areal cover change analysis for Lawas, Terengganu and Kelantan of Malaysia," *Cont. Shelf. Res.* **110**, 124-148 (2015).
- [3] Knudby, A. and Nordlund, L., "Remote sensing of seagrasses in a patchy multi-species environment," *Int. J. Remote Sens.* **32**, 2227-2244 (2011).
- [4] Nordlund, L. M., Koch, E. W., Barbier, E. B. and Creed, J. C., "Seagrass ecosystem services and their variability across genera and geographical regions," *PLoS One* **11**, 1-23 (2016).
- [5] Mumby, P. J., Green, E. P., Edwards, A. J. and Clark, C. D., "The cost-effectiveness of remote sensing for tropical coastal resources assessment and management," *J. Environ. Manag.* **55**, 157-166 (1999).
- [6] Dekker, A., Brando, V., Anstee, J., Fyfe, S., Malthus, T. and Karpouzli E., "Remote sensing of seagrass ecosystems: Use of spaceborne and airborne sensors," Springer Netherlands, 347-359 (2007).

- [7] Borfecchia, F., Cecco, L. De, Martini, S., Ceriola, G., Bollanos, S., Vlachopoulos, G., Valiante, L. M., Belmonte, A. and Micheli, C., "Posidonia oceanica genetic and biometry mapping through high-resolution satellite spectral vegetation indices and sea truth calibration," *Int. J. Remote Sens.* **34**, 4680–4701 (2013).
- [8] Fornes, A., Basterretxea, G., Orfila, A., Jordi, A., Alvarez, A. and Tintore, J., "Mapping Posidonia oceanica from IKONOS," *ISPRS J. Photogramm. Remote Sens.* **60** (5), 315–322 (2006).
- [9] Matta, E., Aiello, M., Bresciani, M., Gianinetto, M., Musanti, M. and Giardino, C., "Mapping Posidonia Meadow From High Spatial Resolution Images in the Gulf of Oristano (Italy)," *IEEE*, Quebec City, 5152–5155 (2014).
- [10] Pasqualini, V., Pergent-Martini, C., Pergent, G., Agreil, M., Skoufas, G., Sourbes, L. and Tsirika, A., "Use of SPOT 5 for mapping seagrasses: an application to Posidonia oceanica," *Remote Sens. Environ.* **94**, 39–45. (2005).
- [11] Rende, S.F., Irving, A. D., Bacci, T., Parlagreco, L., Bruno, F., De Filippo, F., Montefalcone, M., Penna, M., Trabucco, B., Di Mento, R. and Cicero, A. M. "Advances in micro-cartography: a two-dimensional photo mosaicing technique for seagrass monitoring," *Estuar. Coast. Shelf Sci.* **167**, 475-486 (2015).
- [12] Rende, F. S., Irving, A. D., Lagudi A.; Bruno, F., Scalise, S.; Cappa, P., Montefalcone, M., Bacci, T., Penna, M., Trabucco, B., Di Mento, R., Cicero, A. M.," Pilot application of 3D underwater imaging techniques for mapping Posidonia oceanica (L.) Delile meadows,"*ISPRS - Int. Arch Photogramm. Remote Sens. Spat. Inf. Sci.* XL-5/W5, 177-181 (2015).
- [13] Lyzenga, D. R., "Remote sensing of bottom reflectance and water attenuation parameters in shallow water using aircraft and Landsat data," *Int. J. Remote Sens.* **2**(1), 71-82 (1981).
- [14] Bruce, E. M., Eliot, I. G. and Milton D. J., "Method for assessing the thematic and positional accuracy of seagrass mapping," *Mar. Geod.* **20**:2-3, 175-193 (1997).
- [15] Congalton, R. and Green, K., "Assessing the Accuracy of Remotely Sensed Data: Principles and Practices," Second Edition, CRC Press (2008).
- [16] Traganos, D., & Reinartz, P., "Mapping Mediterranean seagrasses with Sentinel-2 imagery," *Mar. Pollut. Bull.* (2017).
- [17] Topouzelis, K., Charalampis Spondylidis, S., Papakonstantinou, A., & Soulakellis, N., "The use of Sentinel-2 imagery for seagrass mapping: Kalloni Gulf (Lesvos Island-Greece) case study," 12 August 2016, 96881F.
- [18] Kachelriess, D., Wegmann, M., Gollock, M. and Pettorelli, N., "The application of remote sensing for marine protected area management," *Ecol. Indic.* **36**, 169-177 (2014).